

How many quantum phase transitions exist inside the superconducting dome of the iron pnictides?

Rafael M. Fernandes,¹ Saurabh Maiti,² Peter Wölfle,³ and Andrey V. Chubukov²

¹*School of Physics and Astronomy, University of Minnesota, Minneapolis, MN 55455, USA*

²*Department of Physics, University of Wisconsin-Madison, Madison, Wisconsin 53706, USA*

³*Institute for Condensed Matter Theory and Institute for Nanotechnology,
Karlsruhe Institute of Technology, 76021 Karlsruhe, Germany*

(Dated: March 5, 2018)

Recent experiments on two iron-pnictide families suggest the existence of a single quantum phase transition (QPT) inside the superconducting dome despite the fact that two separate transition lines - magnetic and nematic - cross the superconducting dome at T_c . Here we argue that these two observations are actually consistent. We show, using a microscopic model, that each order coexists with superconductivity for a wide range of parameters, and both transition lines continue into the superconducting dome below T_c . However, at some $T_{\text{merge}} < T_c$, the two transitions merge and continue down to $T = 0$ as a single simultaneous first-order nematic/magnetic transition. We show that superconductivity has a profound effect on the character of this first-order transition, rendering it weakly first-order and allowing strong fluctuations to exist near the QPT.

Introduction. A common theme across different phase diagrams of unconventional superconductors (SC) is the idea of one or more continuous quantum phase transitions (QPT's) under the SC dome [1]. Examples include heavy fermion materials [2, 3], cuprates [4], and iron pnictides [5]. Such QPT is generally associated with a non-superconducting (SC) order which penetrates into the SC dome [4, 6–11]. Direct experimental access to this putative QPT requires killing the SC order, which can be challenging in high-temperature superconductors due to high value of their critical magnetic fields [1]. An alternative is to search for the QPT directly inside the SC dome. However, there is no guarantee that the non-SC continuous phase transition persists down to $T = 0$, as it may become first-order if the SC and non-SC orders do not coexist microscopically [12, 14–16].

In the iron pnictides, measurements of the $T = 0$ SC penetration depth across the phase diagram of $\text{BaFe}_2(\text{As}_{1-x}\text{P}_x)_2$ found a pronounced peak at $x \approx 0.3$ inside the SC dome, consistent with the existence of a single QPT [17]. Because in the phase diagram of this and other iron pnictides, e.g. $\text{Ba}(\text{Fe}_{1-x}\text{Co}_x)_2\text{As}_2$, a spin-density wave (SDW) transition line meets the SC dome near the highest T_c [13, 14], it is natural to identify the observed peak with a magnetic quantum critical point, like in heavy fermions and other materials. However, in the iron pnictides there is not only one, but two separate phase transition lines that cross the SC dome [20, 21]. Besides the SDW transition at T_m , there is also a nematic/structural transition at $T_n > T_m$, below which the tetragonal C_4 symmetry of the system is spontaneously broken down to C_2 [22, 23]. This peculiar feature raises the issue of how many QPTs - if any - exist inside the SC dome.

In this paper we address this issue by using a microscopic electronic model which describes simultaneously the magnetic, nematic, and superconducting phases. We show that SDW and nematic orders coexist with superconductivity such that both the T_m and T_n lines pene-

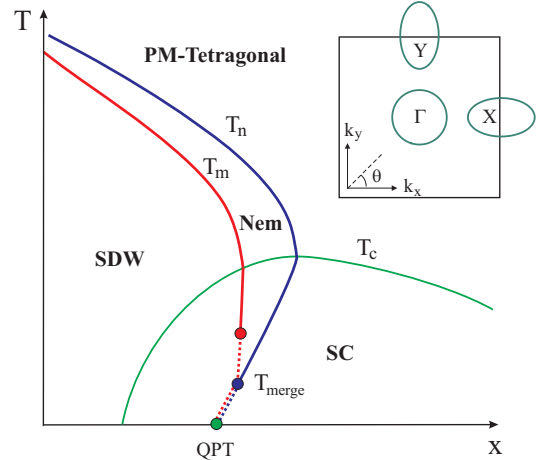


Figure 1: Schematic phase diagram summarizing our main results. The spin-density wave and nematic transition lines, T_m and T_n , separately cross the superconducting transition line, T_c , and coexist with superconductivity immediately below T_c . As temperature is lowered, one of the transitions becomes first-order (dashed line). At a smaller $T = T_{\text{merge}}$ the two transition lines merge onto a single simultaneous weakly first-order transition, which persists down to $T = 0$ and gives rise to a single QPT inside the dome. The back-bending of the lines below T_c may or may not take place (see Refs. [4, 15, 16]). Inset: schematic Fermi surface.

trate separately into the SC dome. However, at $T = 0$, deep inside the SC dome, the nematic and SDW transition lines merge on a *single weakly first-order* QPT (Fig. 1). The weak character of this transition is a direct consequence of the coexistence with SC, and implies the persistence of quantum critical fluctuations for wide temperature and doping ranges, which should affect the macroscopic properties of these materials. Our results also reconcile the existence of two split phase transitions above T_c with the penetration depth measurements of

[17], which point to a single phase transition at $T = 0$ inside the SC dome.

Microscopic model. We consider a minimal model consisting of one circular hole pocket at the center of the 1-Fe Brillouin zone and two elliptical electron pockets centered at momenta $\mathbf{Q}_X = (\pi, 0)$ and $\mathbf{Q}_Y = (0, \pi)$. The band dispersions are parameterized in terms of the momentum k and angle θ as $\varepsilon_{\Gamma, \mathbf{k}} = -\varepsilon_{\mathbf{k}} = \varepsilon_0 - \frac{k^2}{2m}$, $\varepsilon_{X, \mathbf{k}} = \varepsilon_{\mathbf{k} - \mathbf{Q}_X} + 2\delta_0 + 2\delta_2 \cos 2\theta$, and $\varepsilon_{Y, \mathbf{k}} = \varepsilon_{\mathbf{k} - \mathbf{Q}_Y} + 2\delta_0 - 2\delta_2 \cos 2\theta$, where δ_0 is proportional to doping and δ_2 originates from the ellipticity of the electron pockets [22, 24] (see inset in Fig. 1). The Hamiltonian of the model is $H = H_2 + H_4$. The free-fermion part is $H_2 = \sum_{a, \mathbf{k}} (\varepsilon_{a, \mathbf{k}} - \mu) c_{a, \mathbf{k}\sigma}^\dagger c_{a, \mathbf{k}\sigma}$, where σ is a spin index, a is a band index, and μ is the chemical potential. The interaction term H_4 contains eight different 4-fermion interactions [25].

We follow earlier works and assume that SDW magnetism with momentum \mathbf{Q}_X and/or \mathbf{Q}_Y (order parameters $\mathbf{M}_j = \sum_{\mathbf{k}} c_{\Gamma, \mathbf{k}\alpha}^\dagger \sigma_{\alpha\beta} c_{j, \mathbf{k} + \mathbf{Q}_j\beta}$, $j = X, Y$) and s^{+-} superconductivity (order parameters $\Delta_i = \sum_{\mathbf{k}} c_{i, \mathbf{k}\uparrow}^\dagger c_{i, -\mathbf{k}\downarrow}^\dagger$, $i = X, Y, \Gamma$) are the primary instabilities, while nematicity is caused by magnetic fluctuations [22, 26–28]. Decoupling the interaction terms in H_4 and integrating over the fermions, we obtain the effective action $S_{\text{eff}}[\Delta_i, M_j]$ and expand in Δ and M_i :

$$S_{\text{eff}} = a_m (M_X^2 + M_Y^2) + a_s \Delta^2 + \frac{u_m}{2} (M_X^2 + M_Y^2)^2 - \frac{g_m}{2} (M_X^2 - M_Y^2)^2 + \frac{u_s}{2} \Delta^4 + \lambda \Delta^2 (M_X^2 + M_Y^2) \quad (1)$$

with coefficients depending on the interactions and the band parameters (δ_0, δ_2) (see Supplementary Material (SM) for details). The coefficients a_m and a_s vanish at the mean-field SDW and SC transition temperatures $T_{m,0}$ and $T_{c,0}$, while the coefficients $u_m > g_m, u_s$, and λ are all positive at not very low T . Here we considered equal inter-band pairing interactions, implying $\Delta_\Gamma = -\sqrt{2}\Delta_{X,Y} = \Delta$.

Mean-field analysis. We first analyze this action at the mean-field level, when the M and Δ fields do not fluctuate. In this case, although there is no preemptive nematic order, the tetragonal symmetry is broken below $T_{m,0}$, because the minimum of Eq. (1) is a stripe SDW phase with either $M_X = 0, M_Y \neq 0$ or $M_X \neq 0, M_Y = 0$. The competing SC and SDW orders coexist microscopically as long as the quartic coefficients satisfy the condition $\lambda < \sqrt{u_s(u_m - g_m)}$ (Refs.[12, 14–16]). This happens in the light-blue region of the (δ_0, δ_2) space of Fig. 2. [29] For parameters in this range, the continuous SDW transition line penetrates into the SC state, albeit with a different slope [4]. It survives down to $T = 0$ if $u_m > 0$, which is the case when the SC gap is not too small (see SM). In this case, the mean-field SDW transition remains second-order down to $T = 0$ and ends up at a magnetic quantum critical point under the SC dome.

Preemptive nematic order. To include fluctuations of the SDW fields M_X and M_Y we replace a_m in Eq. (1) by the SDW susceptibility $\chi_0^{-1}(\mathbf{Q}_i + \mathbf{q}, \omega_n) = a_m + q^2 +$

$f(\omega_n)$, where $\omega_n = 2\pi nT$ is the Matsubara frequency and $f(\omega_n)$ is proportional to $|\omega_n|$ in the normal state and ω_n^2 deep inside the SC dome. We then introduce two Hubbard-Stratonovich fields $\psi = u_m \langle M_X^2 + M_Y^2 \rangle$ and $\varphi = g_m \langle M_X^2 - M_Y^2 \rangle$, integrate the partition function over $M_i(\mathbf{q}, \omega_n)$, and obtain the effective action $S_{\text{eff}}[\Delta, \psi, \varphi]$. Fluctuations of M_i and of ψ and φ are conjugated - if M_i fluctuates strongly, as we now assume, fluctuations of ψ and φ are weak, and the effective action $S_{\text{eff}}[\Delta, \psi, \varphi]$ can in turn be analyzed in the saddle-point approximation (see SM). The field $\langle \psi \rangle$ is always non-zero and shifts the “pure” SDW transition temperature from $T_{m,0}$ down to $\tilde{T}_{m,0}$. Our analysis, for which we used the expansion to order M^4 in Eq. (1) is valid when $(T_n - \tilde{T}_{m,0})/T_n \leq 1$. A non-zero $\langle \varphi \rangle$ appears only below a certain T_n and breaks the tetragonal C_4 symmetry down to C_2 , inducing an orthorhombic distortion and orbital order [22]. If $\langle \varphi \rangle$ becomes non-zero at $T_n > \tilde{T}_{m,0}$, there exists a temperature range in which the system displays nematic order $\langle \varphi \rangle \neq 0$ but no long-range magnetic order $\langle \mathbf{M}_i \rangle = 0$. In the normal state, the effective action $S_{\text{eff}}[0, \psi, \varphi]$ is

$$S_{\text{eff}}[0, \psi, \varphi] = \frac{\varphi^2}{2g_m} - \frac{\psi^2}{2u_m} + \frac{3}{2} \int_q \log \left[(\chi_0^{-1} + \psi)^2 - \varphi^2 \right] \quad (2)$$

where $\int_q = T \sum_{\omega_n} \int d^d q / (2\pi)^d$. This action has been analyzed before in several contexts [22, 30–36]. For quasi-2D layered systems, the behavior depends on the ratio $\alpha = u_m/g_m \geq 1$. For α relevant to near-optimally doped BaFe₂(As_{1-x}P_x)₂ and Ba(Fe_{1-x}Co_x)₂As₂, the nematic transition is second order and occurs at $T_n > \tilde{T}_{m,0}$, i.e. before the “pure” SDW transition. A non-zero $\langle \varphi \rangle$ shifts the SDW transition upwards from $\tilde{T}_{m,0}$ to T_m , but still $T_m < T_n$. In this situation, there are two split second-order transition lines, T_n and T_m , which separately cross the T_c line. Our goal now is to find the fate of these transitions inside the SC dome.

Coexistence of nematicity and SC. We first consider the vicinity of the point where the nematic transition line T_n hits T_c . For simplicity, we set $d = 2$ to study the coexistence between nematicity and SC. This procedure is safe for the nematic order, as it only breaks a discrete symmetry. Inter-layer coupling will only account for small corrections to T_n , but it is crucial for the existence of an SDW transition line at $\tilde{T}_{m,0} > 0$. We assume that T_c is large enough and neglect the dynamic part of χ_0 . We obtain ψ from the saddle-point equation $\partial S_{\text{eff}} / \partial \psi = 0$, substitute the result back into the effective action and obtain $S_{\text{eff}}[\Delta, \varphi]$:

$$S_{\text{eff}}[\Delta, \varphi] = a_n \varphi^2 + \frac{u_n}{2} \varphi^4 + \tilde{a}_s \Delta^2 + \frac{\tilde{u}_s}{2} \Delta^4 + \tilde{\lambda} \varphi^2 \Delta^2 \quad (3)$$

where :

$$\tilde{\lambda} = \frac{\lambda}{2(u_m + g_m)}, \quad \tilde{u}_s = \frac{u_s - \frac{\lambda^2}{u_m + g_m}}{2g}, \quad u_n = \frac{1}{6} \frac{u_m - 2g_m}{u_m + g_m} \quad (4)$$

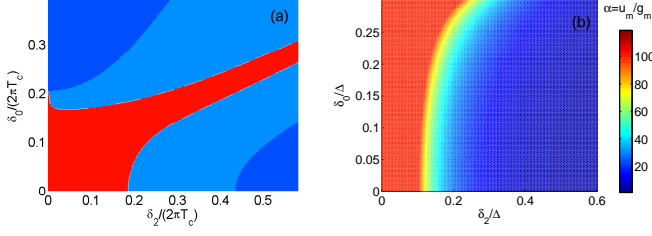


Figure 2: (a) The regions of coexistence between mean-field SDW and superconductivity (light-blue region) and nematicity and superconductivity (red region) in the (δ_0, δ_2) parameter space, in $d = 2$. In the red region both SDW and nematic order coexist with SC order. (b) Color plot of $\alpha = u_m/g_m$ inside the SC state for different δ_0/Δ and δ_2/Δ (Δ is the SC gap).

Notice that all coefficients originate from the SDW/SC action (1), i.e. the coupling between the nematic and SC order parameters is a consequence of the coupling between the SDW and SC fields ($\tilde{\lambda} \propto \lambda$) [26]. In the absence of SC, the nematic transition is second-order when $u_n > 0$, i.e. $\alpha = u_m/g_m > 2$, which we assume to hold.

It follows from Eq. (3) that nematic and SC orders coexist when $\tilde{\lambda} < \sqrt{u_s u_n}$, which in terms of the original Ginzburg-Landau coefficients gives $\lambda < \sqrt{u_s(u_m - 2g_m)}$. Although this is a more restrictive condition than $\lambda < \sqrt{u_s(u_m - g_m)}$ for the coexistence between mean-field SDW and SC, it is still satisfied in a rather wide range of parameters (δ_0, δ_2) , including the region of small δ_0 and δ_2 (the red region in Fig. 2a). In this parameter range, the second-order T_n line continues below T_c , albeit with a different slope. Because the condition for SDW-SC coexistence is the same both in mean-field and in the presence of Gaussian fluctuations [14], in the same red region of Fig. 2a, the SDW T_m line also continues as a second-order transition line into the SC dome.

Nematic and SDW transitions at $T = 0$. At $T = 0$, the dynamics of $\chi_0(\mathbf{q}, \omega_n)$ cannot be neglected. Deep in the SC state, the spin dynamics is propagating $\chi_0^{-1}(\mathbf{Q}_i + \mathbf{q}, \omega_n) = a_m + q^2 + \omega_n^2$, i.e. the quantum system behaves like the classical system in an effective dimension $d_{\text{eff}} = d + 1 = 3$.

The effective action in terms of ψ and φ has the same form as in the absence of SC, Eq. (2), but with renormalized coefficients and in $d_{\text{eff}} = 3$. Anticipating that nematic transition may trigger an instantaneous magnetic transition, we introduce an SDW order parameter m (the average value of either M_X or M_Y , depending on the sign of φ) and write S_{eff} in terms of ψ, φ , and m (Ref. [22]). We again use $\partial S_{\text{eff}}/\partial \psi = 0$ to eliminate ψ and obtain the action in terms of φ and m :

$$S_{\text{eff}}[\varphi, m] = \frac{\varphi^2}{2g_m} - \frac{r(r - 2\bar{a}_m)}{2u_m} + \frac{3}{2\pi}m^2(r - |\varphi|) - \frac{(r + \varphi)^{3/2} + (r - \varphi)^{3/2}}{4\pi} \quad (5)$$

where $r = \bar{a}_m - (3u_m/8\pi)(\sqrt{r + \varphi} + \sqrt{r - \varphi}) + (3u_m/2\pi)m^2$ is a function of φ and m , and $\bar{a}_m = a_m + (3\Lambda u_m)/(2\pi^2)$ is the renormalized distance to the $T = 0$ SDW transition in the absence of nematicity. The magnetic order parameter m satisfies the equation of state $m(r - |\varphi|) = 0$. It vanishes if the nematic order parameter either emerges continuously or jumps to a value $|\varphi| < r$, but can become non-zero if φ jumps at the nematic transition to $|\varphi| = r$. That m can become non-zero right at the nematic transition can also be understood by looking at the SDW susceptibility $\chi(\mathbf{Q}_i) \propto 1/r$. For $\varphi = 0$, the SDW susceptibility diverges when $r = 0$, which happens at $\bar{a}_m = 0$. If the nematic transition occurs at $\bar{a}_m > 0$, preempting the magnetic transition, the static SDW susceptibility splits into $\chi(\mathbf{Q}_i) \propto 1/(r \pm \varphi)$. If φ jumps to $|\varphi| = r$ at the nematic transition, one of the $\chi(\mathbf{Q}_i)$ diverges, and m may also jump.

We analyzed $S_{\text{eff}}[\varphi, m]$ by reducing \bar{a}_m from some initially large positive value in the paramagnetic phase down to $\bar{a}_m = 0$ (at the pure $T = 0$ SDW transition). This is valid for systems where the pure SDW transition is continuously suppressed to zero. In the range, $|\varphi| \leq \varphi_0$, where $\varphi_0 = \frac{1}{32} \left(\sqrt{\frac{9u_m^2}{4\pi^2} + 32\bar{a}_m} - \frac{3u_m}{2\pi} \right)^2$, we have $|\varphi| \leq r$ and hence $m = 0$. For $|\varphi| > \varphi_0$, we have $r = |\varphi|$ and $m(\varphi, \bar{a}_m) \neq 0$ determined from the equation on r . Our results are shown in Fig. 3 where we plotted $S_{\text{eff}}[\varphi]$ in both regions at various \bar{a}_m . For large \bar{a}_m , $S_{\text{eff}}(\varphi)$ has a minimum at $\varphi = 0$ and monotonically increases with $|\varphi|$. When \bar{a}_m becomes smaller than $\bar{a}_{m,c1} = (3u/4\pi)^2/(2(\alpha - 1))$, $S_{\text{eff}}(\varphi)$ develops inflection points at $|\varphi| > \varphi_0$. Upon decreasing \bar{a}_m further, these inflection points split in two pairs of local maximum and minimum $\varphi = \pm\varphi_{\text{max}}$ and $\varphi = \pm\varphi_{\text{min}}$. At some $0 < \bar{a}_{m,cr} \leq \bar{a}_{m,c1}$, $S_{\text{eff}}[\varphi = \pm\varphi_{\text{min}}]$ eventually becomes lower than $S_{\text{eff}}[\varphi = 0]$, i.e. the system undergoes a first-order nematic transition in which the nematic order parameter jumps from $\varphi = 0$ to $\varphi = \pm\varphi_{\text{min}}$. Because $\varphi_{\text{min}} > \varphi_0$, the jump in the nematic order parameter is strong enough to induce a simultaneous first-order magnetic transition. Since at the transition both φ and m jump simultaneously to finite values, there is only one first-order QPT under the SC dome (see Fig. 1).

We verified that at $\bar{a}_{m,cr}$ the coefficient of the φ^2 term in $S_{\text{eff}}[\varphi]$ remains positive for all $\alpha \equiv u_m/g_m$, i.e. the first-order nematic transition preempts not only the SDW transition but also the potential second-order nematic transition. This result is at variance with earlier works (Ref. [31]) which suggested separate second-order transitions at $T = 0$ in $d_{\text{eff}} = 3$.

An important issue is the strength of this first-order transition. For $d_{\text{eff}} = 3$, φ_0 and the jump in the nematic order parameter $\delta\phi$ decreases when α increases and scale as $1/\alpha^2$ at large α . Similarly, $\bar{a}_{m,c1}$, below which the first-order transition preempts the pure SDW QCP, scales as $1/\alpha$. These scalings are a general consequence of the fact that $d_{\text{eff}} = 3$ is the borderline between the regimes of simultaneous and split nematic/SDW transitions, since for

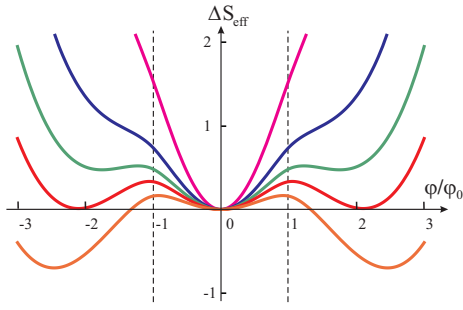


Figure 3: The effective action $S_{\text{eff}}[\varphi]$ at $T = 0$ and $d_{\text{eff}} = 3$, as a function of the nematic order parameter φ for various \bar{a}_m , which measure the distance to the pure SDW $T = 0$ transition. From top to bottom, $\bar{a}_m \left(\frac{4\pi^2}{9u_m^2} \right) = 0.0345, 0.0320, 0.0310, 0.03034, \text{ and } 0.0295$. The dashed line $\varphi = \varphi_0$ separates the region where nematic order does not induce magnetic order ($|\varphi| < \varphi_0$) from the regions where magnetic order is simultaneously induced ($|\varphi| > \varphi_0$). We set $u_m/g_m = 5$.

$d_{\text{eff}} = 3 - \epsilon$ the two transition become split and second-order for $\alpha > \frac{3}{2\epsilon}$. Interestingly, we found that, in a wide region of (δ_0, δ_2) , α becomes large in the SC state (see Fig. 2b), i.e. the presence of superconductivity makes the first-order transition weaker. Note in this regard that the effective dimension $d_{\text{eff}} = 3$ is also a direct consequence of the presence of SC, which changes the spin dynamics to propagating. Without SC, the spin dynamics would be diffusive with $d_{\text{eff}} = 2 + z = 4$, and the first-order transition would be much stronger [37].

The weak character of the first-order QPT inside the SC dome is also manifested in the temperature range $0 < T < T_c$. By combining the present results at $T = 0$ and near T_c with the earlier analysis of the classical phase diagram in quasi-2D systems [22], we find that the nematic and magnetic transition lines merge at some non-zero temperature $T_{\text{merge}} < T_c$, below which the two orders develop simultaneously via a first-order transition (see Fig. 1). The details of the phase diagram near T_{merge} depend on the strength of the inter-layer coupling, with either the nematic or the magnetic transition line becoming second-order immediately above T_{merge} . Most importantly, T_{merge} also scales as $1/\alpha^2$ and is small at large $\alpha = u_m/g_m$. As a result, the system behaves almost like the nematic and SDW second-order transition lines would merge right at $T = 0$. In this special case, stripe and non-stripe magnetic states are degenerate, and the SDW order parameter manifold is enhanced to $O(6)$, i.e. only the modulus of the 6-component vector $(\mathbf{M}_X, \mathbf{M}_Y)$ is fixed. This gives rise to enhanced quantum fluctuations near the QPT.

Comparison with experiments Our results can be

directly applied to iron pnictides, particularly to $\text{BaFe}_2(\text{As}_{1-x}\text{P}_x)_2$ and $\text{Ba}(\text{Fe}_{1-x}\text{Co}_x)_2\text{As}_2$, whose SC domes are crossed by two split second-order magnetic and nematic transition lines. Microscopic coexistence between SDW and superconductivity has been established in both cases by NMR [38–40], and a suppression of the orthorhombic order parameter (proportional to φ in our model) has been found inside the SC dome [20, 21]. Our calculations predict a single simultaneous weak first-order nematic/SDW QPT at $T = 0$, which can be verified by measurements of the $T = 0$ SC penetration depth. In $\text{BaFe}_2(\text{As}_{1-x}\text{P}_x)_2$, a single peak in the penetration depth has been observed near optimal doping [17]. Experiments cannot resolve whether it implies a second-order or weakly first-order transition, but the fact is that there is a single transition at $T = 0$, despite two split transitions crossing into the SC dome, in agreement with our theory. The peak in the penetration depth (but not a divergence) is expected due to $O(3)$ SDW fluctuations [18, 19]. When T_{merge} is small, as it is for large α (see Fig. 2b), the emerging $O(6)$ symmetry further enhances the strength of the peak. In $\text{Ba}(\text{Fe}_{1-x}\text{Co}_x)_2\text{As}_2$, penetration depth measurements have so far not identified a peak inside the SC dome, yet the penetration depth was found to increase below a certain doping [41]. This increase is expected in the SDW+SC phase due to the competition between SC and SDW orders [42, 43], and in this regard the experimental result is again consistent with the existence of a single transition point at $T = 0$.

To summarize, in this paper we considered the behavior of the SDW and nematic transition lines inside the SC dome. We argued that both orders coexist with SC, and the two transition lines separately penetrate into the SC dome as continuous second-order transitions. However, as temperature is lowered, they merge at some small but finite T_{merge} , giving rise to a single nematic/SDW weakly first-order QPT. The weak character of the transition is a direct consequence of the coexistence with the SC order, which makes the spin dynamics propagating and enhances the ratio of the quartic couplings, pushing the system to the borderline between the first-order and second-order regimes.

We thank I. Eremin, M. Khodas, Y. Matsuda, R. Prozorov, S. Sachdev, J. Schmalian, T. Shibauchi, and O. Starykh for fruitful discussions. A.V.C. and S.M. are supported by the DOE grant DE-FG02-ER46900. PW is grateful for the hospitality extended to him as a visiting professor at the University of Wisconsin, Madison, and acknowledges support through an ICAM Senior Scientist Fellowship. SM acknowledges support from ICAM-DMR-084415.

[1] S. Sachdev, *Quantum phase transitions of antiferromagnets and the cuprate superconductors*, Lecture Notes in

Physics v. **843**, Springer, Berlin (2012).
[2] P. Wölfle and E. Abrahams, Phys. Rev. B **84**, 041101(R)

- (2011).
- [3] H. v. Löhneysen, A. Rosch, M. Vojta, and P. Wölfle, *Rev. Mod. Phys.* **79**, 1015 (2007).
 - [4] E. G. Moon and S. Sachdev, *Phys. Rev. B* **82**, 104516 (2010); *Phys. Rev. B* **85**, 184511 (2012).
 - [5] K. Ishida, Y. Nakai, and H. Hosono, *J. Phys. Soc. Jpn.* **78**, 062001 (2009); D. C. Johnston, *Adv. Phys.* **59**, 803 (2010); J. Paglione and R. L. Greene, *Nat. Phys.* **6**, 645 (2010); P. C. Canfield and S. L. Bud'ko, *Annu. Rev. Condens. Matter Phys.* **1**, 27 (2010); H.H. Wen and S. Li, *Annu. Rev. Condens. Matter Phys.* **2**, 121 (2011); P. J. Hirschfeld, M. M. Korshunov, and I. I. Mazin, *Rep. Prog. Phys.* **74**, 124508 (2011); A.V. Chubukov, *Annu. Rev. Condens. Matter Phys.* **3**, 57 (2012).
 - [6] A. Abanov, A. V. Chubukov, and J. Schmalian, *Adv. Phys.* **52**, 119 (2003).
 - [7] M. A. Metlitski and S. Sachdev, *Phys. Rev. B* **82**, 075128 (2010).
 - [8] Y. Wang and A. V. Chubukov, *Phys. Rev. Lett.* **110**, 127001 (2013).
 - [9] H. Meier, C. Pepin and K. B. Efetov, arXiv:1210.3276
 - [10] J.-H. She, B. J. Overbosch, Y.-W. Sun, Y. Liu, K. Schalm, J. A. Mydosh, and J. Zaanen, *Phys. Rev. B* **84**, 144527 (2011).
 - [11] D. J. Scalapino, *Rev. Mod. Phys.* **84**, 1383 (2012)
 - [12] A. B. Vorontsov, M. G. Vavilov, and A. V. Chubukov, *Phys. Rev. B* **79**, 060508(R) (2009).
 - [13] S. Kasahara et al., *Phys. Rev. B* **81**, 184519 (2010).
 - [14] R. M. Fernandes, D. K. Pratt, W. Tian, J. Zarestky, A. Kreyssig, S. Nandi, M. G. Kim, A. Thaler, N. Ni, P. C. Canfield, R. J. McQueeney, J. Schmalian, and A. I. Goldman, *Phys. Rev. B* **81**, 140501(R) (2010).
 - [15] A. B. Vorontsov, M. G. Vavilov, and A. V. Chubukov, *Phys. Rev. B* **81**, 174538 (2010).
 - [16] R. M. Fernandes and J. Schmalian, *Phys. Rev. B* **82**, 014521 (2010).
 - [17] K. Hashimoto, K. Cho, T. Shibauchi, S. Kasahara, Y. Mizukami, R. Katsumata, Y. Tsuruhara, T. Terashima, H. Ikeda, M. A. Tanatar, H. Kitano, N. Salovich, R. W. Giannetta, P. Walmsley, A. Carrington, R. Prozorov, and Y. Matsuda, *Science* **336**, 1554 (2012); K. Hashimoto, Y. Mizukami, R. Katsumata, H. Shishido, M. Yamashita, H. Ikeda, Y. Matsuda, J. A. Schlueter, J. D. Fletcher, A. Carrington, D. Gnida, D. Kaczorowski, and T. Shibauchi *Proc. Natl. Acad. Sci. USA* **110**, 3293-3297 (2013).
 - [18] A. Levchenko, M. G. Vavilov, M. Khodas, and A. V. Chubukov, arXiv:1212.5719; T. Nomoto and H. Ikeda, preprint.
 - [19] D. Chowdhury, B. Swingle, E. Berg, and S. Sachdev, arXiv:1305.2918
 - [20] S. Nandi, M. G. Kim, A. Kreyssig, R. M. Fernandes, D. K. Pratt, A. Thaler, N. Ni, S. L. Bud'ko, P. C. Canfield, J. Schmalian, R. J. McQueeney, and A. I. Goldman, *Phys. Rev. Lett.* **104**, 057006 (2010).
 - [21] A. E. Bohmer, P. Burger, F. Hardy, T. Wolf, P. Schweiss, R. Fromknecht, H. v. Löhneysen, C. Meingast, H. K. Mak, R. Lortz, S. Kasahara, T. Terashima, T. Shibauchi, and Y. Matsuda, *Phys. Rev. B* **86**, 094521 (2012).
 - [22] R. M. Fernandes, A. V. Chubukov, J. Knolle, I. Eremin, and J. Schmalian, *Phys. Rev. B* **85**, 024534 (2012).
 - [23] I. R. Fisher, L. Degiorgi, and Z. X. Shen, *Rep. Prog. Phys.* **74**, 124506 (2011).
 - [24] I. Eremin and A. V. Chubukov, *Phys. Rev. B* **81**, 024511 (2010).
 - [25] S. Maiti and A. V. Chubukov, *Phys. Rev. B* **82**, 214515 (2010).
 - [26] R. M. Fernandes, L. H. VanBebber, S. Bhattacharya, P. Chandra, V. Keppens, D. Mandrus, M. A. McGuire, B. C. Sales, A. S. Sefat, and J. Schmalian, *Phys. Rev. Lett.* **105**, 157003 (2010).
 - [27] C. Fang, H. Yao, W.-F. Tsai, J. Hu, and S. A. Kivelson, *Phys. Rev. B* **77**, 224509 (2008).
 - [28] C. Xu, M. Muller, and S. Sachdev, *Phys. Rev. B* **78**, 020501(R) (2008).
 - [29] Note that in our 3-band model SDW and SC orders coexist at arbitrary δ_0/δ_2 when δ_0 and δ_2 are small enough. In a two-band model, the coexistence in this limit is possible only in some range of δ_0/δ_2 [12, 14–16].
 - [30] V. Barzykin and L.P. Gor'kov, *Phys. Rev. B* **79**, 134510 (2009).
 - [31] Y. Qi and C. Xu, *Phys. Rev. B* **80**, 094402 (2009).
 - [32] A. Cano, M. Civelli, I. Eremin, and I. Paul, *Phys. Rev. B* **82**, 020408(R) (2010).
 - [33] Y. Kamiya, N. Kawashima, and C. D. Batista, *Phys. Rev. B* **84**, 214429 (2011).
 - [34] R. Applegate, R. R. P. Singh, C.-C. Chen, and T. P. Devereaux, *Phys. Rev. B* **85**, 054411 (2012).
 - [35] G. Giovannetti, C. Ortix, M. Marsman, M. Capone, J. van den Brink, and J. Lorenzana, *Nature Comm.* **2**, 398 (2011); M. Capati, M. Grilli, and J. Lorenzana, *Phys. Rev. B* **84**, 214520 (2011).
 - [36] A. J. Millis, *Phys. Rev. B* **81**, 035117 (2010).
 - [37] For $d_{eff} = 4$, the magnitude of the jump in φ is generally of order of the upper cutoff Λ , and gets smaller only for very large α .
 - [38] Y. Laplace, J. Bobroff, F. Rullier-Albenque, D. Colson, and A. Forget, *Phys. Rev. B* **80**, 140501(R) (2009).
 - [39] M.-H. Julien, H. Mayaffre, M. Horvatic, C. Berthier, X. D. Zhang, W. Wu, G. F. Chen, N. L. Wang, and J. L. Luo, *EPL* **87**, 37001 (2009).
 - [40] T. Iye, Y. Nakai, S. Kitagawa, K. Ishida, S. Kasahara, T. Shibauchi, Y. Matsuda, and T. Terashima, *J. Phys. Soc. Jpn.* **81**, 033701 (2012).
 - [41] R. T. Gordon, H. Kim, N. Salovich, R. W. Giannetta, R. M. Fernandes, V. G. Kogan, T. Prozorov, S. L. Bud'ko, P. C. Canfield, M. A. Tanatar, and R. Prozorov, *Phys. Rev. B* **82**, 054507 (2010).
 - [42] R. M. Fernandes and J. Schmalian, *Phys. Rev. B* **82**, 014520 (2010).
 - [43] D. Kuzmanovski and M. G. Vavilov, *Supercond. Sci. Technol.* **25**, 084001 (2012).

Supplementary material for “How many quantum phase transitions exist inside the superconducting dome of the iron pnictides?”

I. DERIVATION OF THE EFFECTIVE ACTIONS

A. Spin-density wave and superconductivity

We consider a model with one hole pocket at the Γ -point and two symmetry-related elliptical electron pockets at the X and Y points of the unfolded Brillouin Zone (BZ). Of the eight electronic interactions present in this model [1], two contribute to the superconducting (SC) and spin-density wave (SDW) channels: the electron-hole density-density interactions (U_1) and electron-hole pair hopping interactions (U_3). The Hamiltonian is given by $H = H_2 + H_4$, with:

$$\begin{aligned} H_2 &= \sum_{\mathbf{k}, i \in (X, Y, \Gamma)} \varepsilon_{\mathbf{k}, i} c_{\mathbf{k}\sigma, i}^\dagger c_{\mathbf{k}\sigma, i} \\ H_4 &= \sum_{\mathbf{k}, i \in (X, Y)} U_1 c_{\mathbf{k}\alpha, \Gamma}^\dagger c_{\mathbf{k}\gamma, i}^\dagger c_{\mathbf{k}\delta, i} c_{\mathbf{k}\beta, \Gamma} \delta_{\alpha\beta} \delta_{\gamma\delta} \\ &\quad + \sum_{k, i \in (X, Y)} \frac{U_3}{2} \left(c_{\mathbf{k}\alpha, \Gamma}^\dagger c_{\mathbf{k}\gamma, \Gamma}^\dagger c_{\mathbf{k}\delta, i} c_{\mathbf{k}\beta, i} + \text{h.c.} \right) \delta_{\alpha\beta} \delta_{\gamma\delta} \end{aligned} \quad (\text{S1})$$

where summation over spin indices is implied. The dispersions $\varepsilon_{\mathbf{k}, i}$ are given in the main text as function of δ_0 (which is proportional to the chemical potential) and δ_2 (which is proportional to the ellipticity of the electron pockets). In H_4 we retain terms only in the spin and the pairing sector and define the staggered spin operators $\mathbf{S}_i = \frac{1}{\sqrt{2}} \sum_{\mathbf{k}} c_{\mathbf{k}\alpha, \Gamma}^\dagger \boldsymbol{\sigma}_{\alpha\beta} c_{\mathbf{k}\beta, i}$ and the pairing operators $b_i = \sum_{\mathbf{k}} c_{\mathbf{k}\uparrow, i} c_{-\mathbf{k}\downarrow, i}$. We can then rewrite H_4 as:

$$H_4 = -(U_1 + U_3) \sum_{i \in (X, Y)} \mathbf{S}_i \cdot \mathbf{S}_i + 2U_3 \sum_{i \in (X, Y)} (b_\Gamma b_i + \text{h.c.}) \quad (\text{S2})$$

After introducing the Hubbard-Stratonovich fields $\mathbf{M}_{(X, Y)}$ for $\mathbf{S}_{(X, Y)}$, Δ_h for b_Γ , and Δ_e for $b_{(X, Y)}$, we obtain the action S as function of the fermionic fields as well as the SDW and SC fluctuating fields (assumed to be homogeneous):

$$S[\Psi, \mathbf{M}_i, \Delta_i] = \frac{2}{(U_1 + U_3)} (M_X^2 + M_Y^2) - \frac{4}{U_3} \Delta_h \Delta_e - \int_k \hat{\Psi}_k^\dagger (i\omega_n - \hat{\mathcal{H}}_{\mathbf{k}}) \hat{\Psi}_k \quad (\text{S3})$$

Here, $k = (\omega_n, \mathbf{k})$, with $\omega_n = (2n + 1)\pi T$ denoting the fermionic Matsubara frequency, and $\int_k = T \sum_{\omega_n} \int \frac{d^d k}{(2\pi)^d}$. The 12-dimensional Nambu operator is given by $\hat{\Psi}_k^\dagger = \left(\psi_{k, \Gamma}^\dagger \quad \psi_{k, X}^\dagger \quad \psi_{k, Y}^\dagger \right)$, with:

$$\psi_{k, i}^\dagger = \left(c_{\mathbf{k}\uparrow, i}^\dagger \quad c_{\mathbf{k}\downarrow, i}^\dagger \quad c_{-\mathbf{k}\uparrow, i} \quad c_{-\mathbf{k}\downarrow, i} \right) \quad (\text{S4})$$

and:

$$\hat{\mathcal{H}}_{\mathbf{k}} = \begin{pmatrix} \varepsilon_\Gamma & -\Delta_h(i\sigma_y) & -\mathbf{M}_X \cdot \boldsymbol{\sigma} & 0 & -\mathbf{M}_Y \cdot \boldsymbol{\sigma} & 0 \\ \Delta_h(i\sigma_y) & -\varepsilon_\Gamma & 0 & \mathbf{M}_X \cdot \boldsymbol{\sigma}^* & 0 & \mathbf{M}_Y \cdot \boldsymbol{\sigma}^* \\ -\mathbf{M}_X \cdot \boldsymbol{\sigma} & 0 & \varepsilon_X & -\Delta_e(i\sigma_y) & 0 & 0 \\ 0 & \mathbf{M}_X \cdot \boldsymbol{\sigma}^* & \Delta_e(i\sigma_y) & -\varepsilon_X & 0 & 0 \\ -\mathbf{M}_Y \cdot \boldsymbol{\sigma} & 0 & 0 & 0 & \varepsilon_Y & -\Delta_e(i\sigma_y) \\ 0 & \mathbf{M}_Y \cdot \boldsymbol{\sigma}^* & 0 & 0 & \Delta_e(i\sigma_y) & -\varepsilon_Y \end{pmatrix} \quad (\text{S5})$$

Following Ref. [2], we integrate out the fermions and expand for small \mathbf{M} , Δ , obtaining the effective action

$$S_{\text{eff}}[\mathbf{M}_i, \Delta_i] = \frac{2}{(U_1 + U_3)} (M_X^2 + M_Y^2) - \frac{4}{U_3} \Delta_h \Delta_e \\ + \frac{1}{2} \int \text{Tr} (\hat{G}_0 \hat{V})^2 + \frac{1}{2} \int \text{Tr} (\hat{G}_0 \hat{V})^4 + \mathcal{O}(V^6)$$

where $\hat{G}_0 = \text{diag}(G_\Gamma, \tilde{G}_\Gamma, G_X, \tilde{G}_X, G_Y, \tilde{G}_Y)$ and \hat{V} is the same as $\hat{\mathcal{H}}$ but with the diagonal entries set to zero. Here, we introduced the non-interacting Green's functions. $G_{i,k}^{-1} = i\omega - \varepsilon_i$ and $\tilde{G}_{i,k}^{-1} \equiv -G_{i,-k}^{-1} = i\omega + \varepsilon_i$. To simplify our analysis, we consider the s^{+-} SC gap structure given by the solution of the linearized gap equations, which gives $\Delta_e/\Delta_h = -\frac{1}{\sqrt{2}}$. We obtain:

$$S_{\text{eff}}[\mathbf{M}_i, \Delta_i] = a_m (M_X^2 + M_Y^2) + a_s \Delta^2 + \frac{u_s}{2} \Delta^4 \\ + \frac{u_m^{(1)} + u_m^{(2)}}{4} (M_X^2 + M_Y^2)^2 - \frac{u_m^{(2)} - u_m^{(1)}}{4} (M_X^2 - M_Y^2)^2 + \lambda (M_X^2 + M_Y^2) \Delta^2 \quad (\text{S6})$$

with $\Delta_h \equiv \Delta$ and Ginzburg-Landau coefficients:

$$a_m = \frac{2}{(U_1 + U_3)} + 2 \int_k G_\Gamma G_X \\ a_s = \frac{4}{\sqrt{2}U_3} + 2 \int_k (G_\Gamma \tilde{G}_\Gamma + G_X \tilde{G}_X) \\ u_m^{(1)} = \int_k G_\Gamma^2 G_X^2 \\ u_m^{(2)} = \int_k G_\Gamma^2 G_X G_Y \\ \lambda = 2 \int_k \left(G_\Gamma^2 \tilde{G}_\Gamma G_X + \frac{1}{2} G_X^2 \tilde{G}_X G_\Gamma - \frac{1}{\sqrt{2}} G_\Gamma \tilde{G}_\Gamma G_X \tilde{G}_X \right) \\ u_s = 2 \int_k \left(G_\Gamma^2 \tilde{G}_\Gamma^2 + \frac{1}{2} G_X^2 \tilde{G}_X^2 \right) \quad (\text{S7})$$

Evaluating the momentum integrals above give:

$$\int_k G_\Gamma G_X = -2\pi\rho_F T \sum_{n>0} \left\langle \frac{\omega_n}{\omega_n^2 + \tilde{\mu}_X^2} \right\rangle \\ \int_k (G_\Gamma \tilde{G}_\Gamma + G_X \tilde{G}_X) = -4\pi\rho_F T \sum_{n>0} \frac{1}{\omega_n} \\ \int_k G_\Gamma^2 G_X^2 = \pi\rho_F T \sum_{n>0} \left\langle \frac{\omega_n(\omega_n^2 - 3\tilde{\mu}_X^2)}{(\omega_n^2 + \tilde{\mu}_X^2)^3} \right\rangle \\ \int_k G_\Gamma^2 G_X G_Y = \pi\rho_F T \sum_{n>0} \left\langle \frac{\omega_n [(\omega_n^2 - \tilde{\mu}_X \tilde{\mu}_Y)^2 - \tilde{\mu}_X \tilde{\mu}_Y (\tilde{\mu}_X + \tilde{\mu}_Y)^2]}{(\omega_n^2 + \tilde{\mu}_X^2)^2 (\omega_n^2 + \tilde{\mu}_Y^2)^2} \right\rangle \\ \int_k G_\Gamma^2 \tilde{G}_\Gamma^2 = \int_k G_X^2 \tilde{G}_X^2 = \pi\rho_F T \sum_{n>0} \frac{1}{\omega_n^3} \\ \int_k G_X^2 \tilde{G}_X G_\Gamma = \int_k G_\Gamma^2 \tilde{G}_\Gamma G_X = \pi\rho_F T \sum_{n>0} \left\langle \frac{\omega_n}{(\omega_n^2 + \tilde{\mu}_X^2)^2} \right\rangle \\ \int_k G_\Gamma \tilde{G}_\Gamma G_X \tilde{G}_X = \pi\rho_F T \sum_{n>0} \left\langle \frac{1}{\omega_n(\omega_n^2 + \tilde{\mu}_X^2)} \right\rangle$$

where ρ_F is the density of states at the Fermi level, $\langle \rangle$ refers to angular averaging over the Fermi surface, and $\tilde{\mu}_{(X,Y)} = \delta_0 \pm \delta_2 \cos 2\theta$.

B. Nematicity and superconductivity

From Eq.S6, we can follow the steps in Ref. [2] explained in the main text and introduce the new Hubbard-Stratonovic fields φ and ψ corresponding to $M_X^2 + M_Y^2$ (thermal fluctuations) and $M_X^2 - M_Y^2$ (nematic order parameter). After integrating out the Gaussian magnetic fluctuations in the paramagnetic phase, the new effective action is

$$\tilde{S}_{\text{eff}} = \frac{\varphi^2}{2g_m} - \frac{\psi^2}{2u_m} + a_s \Delta^2 + \frac{u_s}{2} \Delta^4 + \frac{N}{2} \int_k \ln [(\psi + \lambda \Delta^2 + \chi_0^{-1})^2 - \varphi^2]$$

where $u_m \equiv \frac{u_m^{(1)} + u_m^{(2)}}{2}$, $g_m \equiv \frac{u_m^{(2)} - u_m^{(1)}}{2}$, and N is the number of components of the magnetic order parameter. Here, $\chi_0^{-1}(\mathbf{Q}_i + \mathbf{q}, \omega_n) = a_m + q^2 + f(\Omega_n)$, where $\Omega_n = 2\pi nT$ is the Matsubara frequency and $f(\Omega_n)$ is proportional to $|\Omega_n|$ in the normal state and Ω_n^2 deep inside the SC state. At the temperature where the nematic transition meets the SC transition line, we can restrict our analysis to $\Omega_n = 0$. Furthermore, since the pnictides are layered materials, we focus here in the case $d = 2$, which gives:

$$\int \frac{d^2 q}{(2\pi)^2} \ln [(r + q^2)^2 - \varphi^2] = \frac{1}{4\pi} [2r(1 + \ln \Lambda^2) - (r + \varphi) \ln(r + \varphi) - (r - \varphi) \ln(r - \varphi)]$$

where Λ is the upper momentum cutoff and we defined $r \equiv \psi + \lambda \Delta^2 + a_m$. To proceed with the saddle point approximation, we rescale $\Delta^2 \rightarrow n \Delta^2$ as well as the quartic coefficients

$$(u_m, u_s, g_m, \lambda) \rightarrow \frac{(u_m, u_s, g_m, \lambda)}{n} \quad (\text{S8})$$

where $n = \frac{NT_c}{8\pi}$. Then, \tilde{S}_{eff} acquires an overall factor of n , rendering the saddle-point approximation exact in the limit $N \rightarrow \infty$. It follows that:

$$\frac{\tilde{S}_{\text{eff}}}{2g_m n} = \varphi^2 - \frac{\psi^2}{2u_m} + a_s \Delta^2 + \frac{u_s}{2} \Delta^4 + r \ln \left(\frac{\Lambda^4}{r^2 - \varphi^2} \right) + 2r - \varphi \ln \left(\frac{r + \varphi}{r - \varphi} \right)$$

where, for convenience, we performed one additional rescaling:

$$(u_m, u_s, \lambda, a_m, a_s, \varphi, \psi, r, \Lambda^2) \rightarrow 2g_m (u_m, u_s, \lambda, a_m, a_s, \varphi, \psi, r, \Lambda^2) \quad (\text{S9})$$

Using the saddle-point equation $\frac{\partial \tilde{S}}{\partial \psi} = 0$, we can eliminate r , which is given implicitly as a function of φ and Δ :

$$r = \bar{a}_m + \lambda \Delta^2 - u_m \ln(r^2 - \varphi^2) \quad (\text{S10})$$

Furthermore, the cutoff Λ has been absorbed into a redefinition of the quadratic term, $\bar{a}_m = a_m + 2u_m \ln \Lambda^2$. The action then can be written as:

$$\bar{S} \equiv \frac{\tilde{S}_{\text{eff}}}{2g_m n} = \varphi^2 + \frac{r^2}{2u_m} + 2r - \varphi \ln \left(\frac{r + \varphi}{r - \varphi} \right) + \left(a_s - \frac{\lambda a_m}{u_m} \right) \Delta^2 + \left(\frac{u_s}{2} - \frac{\lambda^2}{2u_m} \right) \Delta^4 \quad (\text{S11})$$

Since we are interested in the region of the phase diagram where the nematic transition line crosses the SC dome, we expand the action for small φ and Δ . In particular, we substitute in Eq. (S10):

$$r = r_0 + b_1 \varphi^2 + b_2 \varphi^4 + c_1 \Delta^2 + c_2 \Delta^4 + d \varphi^2 \Delta^2 \quad (\text{S12})$$

where r_0 is the solution with $\varphi = 0$, $\Delta = 0$, and find the coefficients b_i , c_i , and d . Substituting this form in \bar{S} and expanding for small φ and Δ , we obtain:

$$\bar{S} = a_n \varphi^2 + \frac{u_n}{2} \varphi^4 + \tilde{a}_s \Delta^2 + \frac{\tilde{u}_s}{2} \Delta^4 + \tilde{\lambda} \varphi^2 \Delta^2$$

with the Ginzburg-Landau coefficients:

$$\begin{aligned}
\tilde{a}_s &= a_s - \frac{\lambda}{u_m} (a_m - r_0) \\
a_n &= 1 - \frac{1}{r_0} \\
\tilde{\lambda} &= \frac{\lambda}{r_0 (r_0 + 2u_m)} \\
\frac{\tilde{u}_s}{2} &= \frac{u_s}{2} - \frac{\lambda^2}{r_0 + 2u_m} \\
\frac{u_n}{2} &= \frac{(-r_0 + u_m)}{6r_0^3 (r_0 + 2u_m)}
\end{aligned} \tag{S13}$$

Since we consider the vicinity of the nematic transition, where $a_n = 0$, we can set $r_0 = 1$ in the quartic coefficients $\tilde{\lambda}$, \tilde{u}_s , and u_n . Going back to the original variables via Eqs. (S8) and (S9), we then obtain the results in Eq. (4) of the main text.

II. SPIN-DENSITY WAVE TRANSITION INSIDE THE SC DOME

To obtain the SDW action deep inside the SC state, where the SC gap Δ is nearly saturated, we go back to the original action (S3) and treat Δ as a parameter, expanding only in powers of M_i :

$$S_{\text{eff}}^{(\text{SC})} [\mathbf{M}_i] = a_m (M_X^2 + M_Y^2) + \frac{u_m^{(1)} + u_m^{(2)}}{4} (M_X^2 + M_Y^2)^2 - \frac{u_m^{(2)} - u_m^{(1)}}{4} (M_X^2 - M_Y^2)^2 \tag{S14}$$

As a result of this procedure, the Ginzburg-Landau coefficients depend now not only on the modified normal Green's function $G_{i,k}$, but also on the anomalous Green's function $F_{i,k}$:

$$\begin{aligned}
G_{i,k} &= -\frac{i\omega_n + \varepsilon_{\mathbf{k},i}}{\omega_n^2 + \varepsilon_{\mathbf{k},i}^2 + \Delta_i^2} \\
F_{i,k} &= \frac{\Delta_i}{\omega_n^2 + \varepsilon_{\mathbf{k},i}^2 + \Delta_i^2}
\end{aligned} \tag{S15}$$

In particular, we obtain:

$$\begin{aligned}
a_m &= \frac{1}{4(U_1 + U_3)} + 2 \int_k (F_\Gamma F_X + G_\Gamma G_X) \\
u_m^{(1)} &= \int_k \left[4F_\Gamma F_X G_\Gamma G_X + F_\Gamma^2 (F_X^2 + G_X \tilde{G}_X) + F_X^2 G_\Gamma \tilde{G}_\Gamma + G_\Gamma^2 G_X^2 \right] \\
u_m^{(2)} &= \int_k \left[F_\Gamma^2 (F_X F_Y + \tilde{G}_X G_Y) + G_\Gamma^2 G_X G_Y + G_\Gamma \tilde{G}_\Gamma F_X F_Y + 4F_\Gamma F_X G_\Gamma G_Y \right]
\end{aligned} \tag{S16}$$

where $\tilde{G}_{i,k} = -G_{i,-k}$. We define the quasi-particle excitation energy $E_i = \sqrt{\Delta_i^2 + \varepsilon_i^2}$ and consider the $T = 0$ limit, where the Matsubara sum becomes an integral over frequencies. Performing this integration yields:

$$\int_k (G_\Gamma G_X + F_\Gamma F_X) = \int_{\mathbf{k}} \frac{1}{2(E_\Gamma + E_X)} \left[-1 + \frac{\varepsilon_\Gamma \varepsilon_X + \Delta_\Gamma \Delta_X}{E_\Gamma E_X} \right] \tag{S17}$$

$$\int_k G_\Gamma G_X F_\Gamma F_X = \int_{\mathbf{k}} \frac{1}{4(E_\Gamma + E_X)^3} \left[-\frac{\Delta_\Gamma \Delta_X}{E_\Gamma E_X} + \frac{\Delta_\Gamma \Delta_X \varepsilon_\Gamma \varepsilon_X}{(E_\Gamma E_X)^2} \Xi \right] \tag{S18}$$

$$\int_k F_\Gamma^2 F_X^2 = \int_{\mathbf{k}} \frac{1}{4(E_\Gamma + E_X)^3} \left(\frac{\Delta_\Gamma \Delta_X}{E_\Gamma E_X} \right)^2 \Xi \tag{S19}$$

$$\int_k \left(F_X^2 G_\Gamma \tilde{G}_\Gamma + F_\Gamma^2 G_X \tilde{G}_X \right) = \int_k \frac{1}{4(E_\Gamma + E_X)^3} \left[-\frac{\Delta_\Gamma^2 + \Delta_X^2}{E_\Gamma E_X} - \frac{\Delta_\Gamma^2 \varepsilon_X^2 + \Delta_X^2 \varepsilon_\Gamma^2}{(E_\Gamma E_X)^2} \Xi \right] \quad (\text{S20})$$

$$\int_k G_\Gamma^2 G_X^2 = \int_k \frac{1}{4(E_\Gamma + E_X)^3} \left[1 - \frac{\varepsilon_\Gamma^2 + \varepsilon_X^2 + 4\varepsilon_\Gamma \varepsilon_X}{E_\Gamma E_X} + \left(\frac{\varepsilon_X \varepsilon_\Gamma}{E_\Gamma E_X} \right)^2 \Xi \right] \quad (\text{S21})$$

where $\Xi = 3 + \frac{E_\Gamma^2 + E_X^2}{E_\Gamma E_X}$. We also obtain:

$$\int_k F_\Gamma^2 F_X F_Y = \int_k \frac{\Delta_\Gamma^2 \Delta_X^2}{E_\Gamma^2} \frac{\mathcal{A} + \mathcal{B}}{\mathcal{D}} \quad (\text{S22})$$

$$\int_k F_\Gamma^2 \tilde{G}_X G_Y = \int_k -\Delta_\Gamma^2 \frac{\mathcal{C} + \mathcal{F}}{\mathcal{D}} - \frac{\Delta_\Gamma^2 \varepsilon_X \varepsilon_Y}{E_\Gamma^2} \frac{\mathcal{A} + \mathcal{B}}{\mathcal{D}} \quad (\text{S23})$$

$$\int_k F_X F_Y \tilde{G}_\Gamma G_\Gamma = \int_k -\Delta_X^2 \frac{\mathcal{C} + \mathcal{F}}{\mathcal{D}} - \frac{\Delta_X^2 \varepsilon_\Gamma^2}{E_\Gamma^2} \frac{\mathcal{A} + \mathcal{B}}{\mathcal{D}} \quad (\text{S24})$$

$$\int_k G_\Gamma G_Y F_\Gamma F_X = \int_k -\Delta_X \Delta_\Gamma \frac{\mathcal{C} + \mathcal{F}}{\mathcal{D}} + \frac{\Delta_\Gamma \Delta_X \varepsilon_\Gamma \varepsilon_Y}{E_\Gamma^2} \frac{\mathcal{A} + \mathcal{B}}{\mathcal{D}} \quad (\text{S25})$$

$$\int_k G_\Gamma^2 G_X G_Y = \int_k \frac{1}{2E_X E_Y (E_X + E_Y)} - (\varepsilon_\Gamma^2 + 2\varepsilon_\Gamma (\varepsilon_X + \varepsilon_Y) + \varepsilon_X \varepsilon_Y + 2E_\Gamma^2) \frac{\mathcal{C} + \mathcal{F}}{\mathcal{D}} + \frac{\varepsilon_\Gamma^2 \varepsilon_X \varepsilon_Y - E_\Gamma^4}{E_\Gamma^2} \frac{\mathcal{A} + \mathcal{B}}{\mathcal{D}} \quad (\text{S26})$$

with:

$$\begin{aligned} \mathcal{A} &= E_\Gamma (E_\Gamma + E_X + E_Y) (2E_\Gamma + E_X + E_Y) \\ \mathcal{B} &= (E_\Gamma + E_X) (E_\Gamma + E_Y) (E_X + E_Y) \\ \mathcal{C} &= (E_\Gamma + E_X + E_Y) (-E_\Gamma^2 + E_X E_Y) \\ \mathcal{F} &= E_\Gamma (E_\Gamma + E_X) (E_Y + E_X) \\ \mathcal{D} &= 4E_\Gamma E_X E_Y (E_\Gamma + E_X)^2 (E_\Gamma + E_Y)^2 (E_X + E_Y) \end{aligned} \quad (\text{S27})$$

Following Ref. [1], we set $\Delta_\Gamma = \Delta$ and $\Delta_X = -\Delta/\sqrt{2}$. The nature of the mean-field SDW transition inside the SC dome is determined by the quartic coefficients $u_m \equiv \frac{u_m^{(1)} + u_m^{(2)}}{2}$, $g_m \equiv \frac{u_m^{(2)} - u_m^{(1)}}{2}$. In the absence of SC, $u_m < 0$ always at $T = 0$, regardless of the band structure parameters δ_0 and δ_2 , implying that at $T = 0$ the SDW transition is first-order. This is illustrated in Fig. S1a, where we plot the $T = 0$ value of u_m given by Eq. (S7) - i.e. without SC - as function of δ_0/ε_F (ε_F is the fermi energy) for $\delta_2 = 0$. The presence of SC can significantly change this result: in Fig. S1b, we plot u_m at $T = 0$ in the presence of SC, as given by Eq. (S16), as function of δ_0/Δ for $\delta_2 = 0$. Clearly, for a large enough SC gap Δ , u_m changes sign, yielding a second-order SDW transition at $T = 0$ as long as $g_m < u_m$ as well. In Fig. 2 of the main text, we plot the $T = 0$ value of the ratio $\alpha = u_m/g_m$ in the entire (δ_0, δ_2) parameter space.

III. NEMATIC TRANSITION INSIDE THE SC DOME

By using the magnetic action inside the SC state, Eq. (S14), with Ginzburg-Landau coefficients renormalized by the SC order, we can go beyond mean-field to study the nematic transition temperature near $T = 0$. In the main text, we showed that at $T = 0$ and $d = 2$, $z = 1$, there is a simultaneous first-order SDW/nematic transition. We now extend this analysis to finite temperatures. Repeating the same procedure as described in Section IB, we introduce the Hubbard-Stratonovich fields φ and ψ and obtain the saddle-point equations:

$$\begin{aligned} \frac{\varphi}{\bar{g}_m} &= 2T \sum_n \int q dq \left(\frac{1}{\psi + a_m + q^2 + \Omega_n^2 - \varphi} - \frac{1}{\psi + a_m + q^2 + \Omega_n^2 + \varphi} \right) \\ \frac{\psi}{\bar{u}_m} &= 2T \sum_n \int q dq \left(\frac{1}{\psi + a_m + q^2 + \Omega_n^2 - \varphi} + \frac{1}{\psi + a_m + q^2 + \Omega_n^2 + \varphi} \right) \end{aligned} \quad (\text{S28})$$

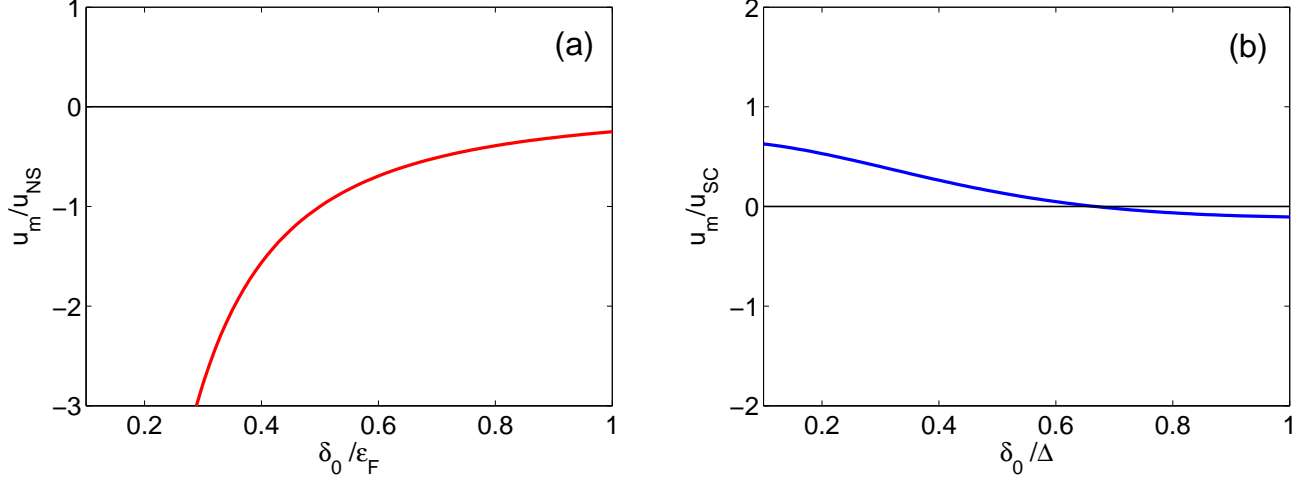


Figure S1: Plot of the $T = 0$ coefficient u_m (a) in the absence of SC (in units of $u_{NS} \equiv \frac{\rho_F}{\varepsilon_F}$, where ε_F is the fermi energy) and (b) in the presence of SC (in units of $u_{SC} \equiv \frac{\rho_F}{\Delta^2}$) as a function of the band dispersion parameter δ_0 . We set $\delta_2 = 0$ in these plots.

where $(\bar{g}_m, \bar{u}_m) = \frac{N}{8\pi} (g_m, u_m)$. To perform the Matsubara frequency summation, we use the identity

$$T \sum_n f(i\Omega_n) = \int_{-\infty}^{\infty} \frac{dx}{2\pi} \coth\left(\frac{x}{2T}\right) \text{Im}[f(x)] \quad (\text{S29})$$

valid for any function f of bosonic Matsubara frequencies $\Omega_n = 2n\pi T$. After defining $r = a_m + \psi$ and the rescaled quantities $(\bar{\varphi}, \bar{r}) = (\bar{\varphi}, \bar{r}) \bar{g}_m^2$, $T = \bar{T} \bar{g}_m$, we obtain the saddle-point equations:

$$\bar{\varphi} = 2\bar{T} \left(\ln \sinh \frac{\sqrt{\bar{r} + \bar{\varphi}}}{2\bar{T}} - \ln \sinh \frac{\sqrt{\bar{r} - \bar{\varphi}}}{2\bar{T}} \right) \quad (\text{S30})$$

$$\bar{r} = \bar{a}_m - 2\bar{T}\alpha \left(\ln \sinh \frac{\sqrt{\bar{r} + \bar{\varphi}}}{2\bar{T}} + \ln \sinh \frac{\sqrt{\bar{r} - \bar{\varphi}}}{2\bar{T}} \right) \quad (\text{S31})$$

where $\bar{a}_m = (a_m + 2\Lambda_q \bar{u}_m) / \bar{g}_m^2$, Λ_q is the momentum integration upper cutoff, and $\alpha = u_m / g_m$. In Fig. S2, we plot the renormalized control parameter \bar{a}_m as function of $\bar{\varphi}$ for different fixed temperatures. We see that for small \bar{T} the first instability (corresponding to the largest \bar{a}_m) is at $0 < \bar{\varphi} < \bar{r}$, indicating a first-order nematic transition. As \bar{T} increases, the first instability moves towards $\bar{\varphi} = 0$, indicating a second-order nematic transition. Because here we considered $d = 2$, the magnetic transition only happens at zero temperature, but for an anisotropic quasi-2D system, following Ref. [2], the magnetic transition will remain first-order and simultaneous to the nematic transition up to a temperature T_{merge} , above which one of the two transition become second-order and split from the other.

IV. ON THE PECULIARITIES OF THE HUBBARD-STRATONOVICH TRANSFORMATION

In this section we discuss one subtle issue related to the regularization of the integrals in the Hubbard-Stratonovich transformation. Consider for instance the transformation from an effective action for the SDW fields Δ_X and Δ_Y deep inside the SC state, Eq. (S14). In the notation we introduced after Eq. (S14),

$$S_{\text{eff}}[\mathbf{M}_i] = a_m (M_X^2 + M_Y^2) + \frac{u_m}{2} (M_X^2 + M_Y^2)^2 - \frac{g_m}{2} (M_X^2 - M_Y^2)^2 \quad (\text{S32})$$

As we discussed above, in the SC state u_m and g_m are both positive. The partition function, from which we extract the free energy, is given by $Z = \int dM_X dM_Y e^{-S_{\text{eff}}[\mathbf{M}_i]}$. The rationale behind the Hubbard-Stratonovich transformation is to rewrite the partition function as an integral over the new fields ψ and φ which describe the

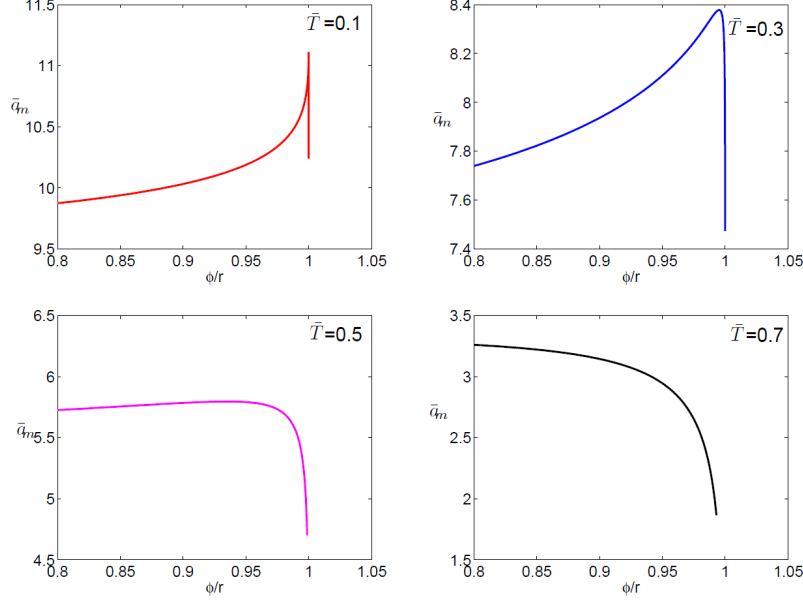


Figure S2: Plot of \bar{a}_m as a function of $\phi/r = \bar{\varphi}/\bar{r}$ inside the SC dome for different temperatures.

fluctuations of $M_X^2 + M_Y^2$ and $M_X^2 - M_Y^2$, respectively. This is done by expressing the quartic terms in $e^{-S_{\text{eff}}[\mathbf{M}_i]}$ as integrals over the new fields ψ and φ of some new effective action $S_{\text{eff}}(M_i, \psi, \varphi)$ which depends only linearly on $M_X^2 + M_Y^2$ and $M_X^2 - M_Y^2$. The integrals over M_X and M_Y in the partition function can then be easily evaluated. Exponentiating the result one expresses the partition function as $Z = \int d\psi d\varphi e^{-S_{\text{eff}}[\psi, \varphi]}$.

For the nematic field φ , the computational procedure is free from subtleties. We use the mathematical identity which states that $e^{\frac{ax^2}{2}}$ can be expressed, for positive a , as

$$e^{\frac{ax^2}{2}} = \frac{1}{\sqrt{2\pi a}} \int_{-\infty}^{\infty} dy e^{\frac{-y^2}{2a} + xy} \quad (\text{S33})$$

Indeed,

$$\int_{-\infty}^{\infty} dy e^{\frac{-y^2}{2a} + xy} = \int_{-\infty}^{\infty} dy e^{\frac{-(y-ax)^2}{2a}} e^{\frac{ax^2}{2}}, \quad (\text{S34})$$

and the integral over y converges and can be trivially evaluated by shifting variables:

$$\int_{-\infty}^{\infty} dy e^{\frac{-(y-ax)^2}{2a}} = 2 \int_0^{\infty} dy e^{-y^2/(2a)} = \sqrt{2\pi a} \quad (\text{S35})$$

Applying this transformation to the g_m term in $e^{-S_{\text{eff}}^{\text{SC}}[\mathbf{M}_i]}$, we obtain:

$$e^{\frac{g_m}{2}(M_X^2 - M_Y^2)^2} = \frac{1}{\sqrt{2\pi g_m}} \int_{-\infty}^{\infty} d\varphi e^{\frac{-\varphi^2}{2g_m} + \varphi(M_X^2 - M_Y^2)} \quad (\text{S36})$$

For the u_m term, however, the Hubbard-Stratonovich transformation is trickier because the corresponding term in the effective action is

$$e^{-\frac{u_m}{2}(M_X^2 + M_Y^2)^2} \quad (\text{S37})$$

where, as we said, $u_m > 0$. We can still formally apply the Hubbard-Stratonovich transformation and obtain

$$e^{-\frac{u_m}{2}(M_X^2 + M_Y^2)^2} = \frac{1}{\Lambda} \int_{-\infty}^{\infty} d\psi e^{\frac{\psi^2}{2u_m} + \psi(M_X^2 + M_Y^2)} \quad (\text{S38})$$

but now the normalization factor

$$\Lambda = 2 \int_0^\infty dy e^{\frac{y^2}{2u_m}} \quad (\text{S39})$$

diverges.

One can avoid the divergence by introducing the imaginary field $\psi \rightarrow i\tilde{\psi}$ instead of the real one, i.e., by writing the exact and well-defined relation

$$e^{-\frac{u_m}{2}(M_X^2 - M_Y^2)^2} = \frac{1}{\sqrt{2\pi u_m}} \int_{-\infty}^\infty d\psi e^{\frac{-\tilde{\psi}^2}{2u_m} + i\tilde{\psi}(M_X^2 + M_Y^2)} \quad (\text{S40})$$

However, later in the calculation the effective action is analyzed as a function of $\tilde{\psi}$ in the complex plane[5] and is taken at the position of the extreme along the *imaginary* axis of $\tilde{\psi}$, i.e., one actually returns to real ψ , for which the normalization factor in Eq. (S38) is the issue.

We argue that the more appropriate way to proceed is to consider Λ in Eq. (S39) as the limit

$$\Lambda = \lim_{\delta \rightarrow \pi} \Lambda_\delta \quad (\text{S41})$$

where

$$\Lambda_\delta = 2 \int_0^\infty dy e^{\frac{-y^2 e^{i\delta}}{2u_m}} \quad (\text{S42})$$

The well-behaved integral in (S35) corresponds to $\delta = 0$.

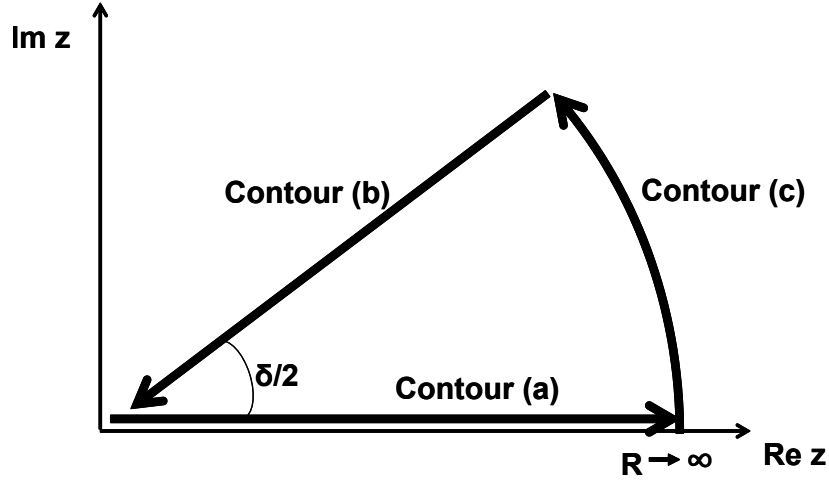


Figure S3: Integration contour for the evaluation of the integral Λ_δ from Eq. (S42). The radius R has to be set to infinity at the end of the calculation.

To evaluate Λ_δ , consider the integral $J_\delta = \oint dz e^{\frac{-z^2 e^{i\delta}}{2}} over a complex variable z , taken over the contour shown in Fig. S3. The contour consists of two lines - one along the positive real axis and one along a line in the upper half-plane of z , directed at an angle $\delta/2$ with respect to the real axis - and the arc with radius R which will be set to infinity at the end of the calculation. We label the corresponding contributions as J_a , J_b , and $\frac{J_c}{2}$, respectively:$

$$\begin{aligned} J_a &= \int_0^R e^{-y^2/2u_m} dy \\ J_b &= -e^{i\delta/2} \int_0^R dy e^{-y^2 e^{i\delta}/(2u_m)} \\ \frac{J_c}{2} &= iR \int_0^{\delta/2} e^{i\theta} e^{-R^2 e^{2i\theta}/(2u_m)} d\theta \end{aligned} \quad (\text{S43})$$

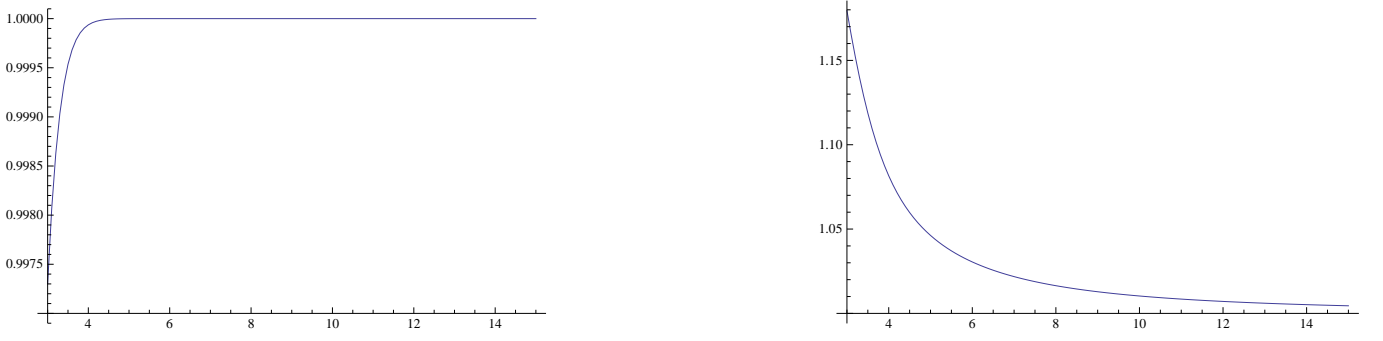


Figure S4: Left and right panels - real and imaginary parts of the integral over the arc of the contour shown in Fig. S3, for θ exactly equal to $\pi/2$, plotted as function of the radius of the arc R . $\text{Re}J_c$ rapidly approaches $-\sqrt{2\pi u_m}$ while $\text{Im}J_c$ approaches $(2u_m/R)e^{R^2/(2u_m)}$. Neither of the integrals oscillates at large R . The vertical axes are $-\text{Re}J_c/\sqrt{2\pi u_m}$ and $\text{Im}J_c(R/2u_m)e^{-R^2/(2u_m)}$, respectively.

The integral J_a is elementary and in the limit of $R \rightarrow \infty$ yields $\sqrt{\pi u_m/2}$. The second integral at $R \rightarrow \infty$ becomes $J_b \rightarrow -(1/2)e^{i\delta/2}\Lambda_\delta$, and the integral J_c over the arc needs to be carefully analyzed.

Because the function $e^{-z^2 e^{i\delta}/2}$ is analytic for any finite z , we have $J = J_a + J_b + J_c = 0$, hence

$$\Lambda_\delta = e^{-i\delta/2} (\sqrt{2\pi u_m} + J_c) \quad (\text{S44})$$

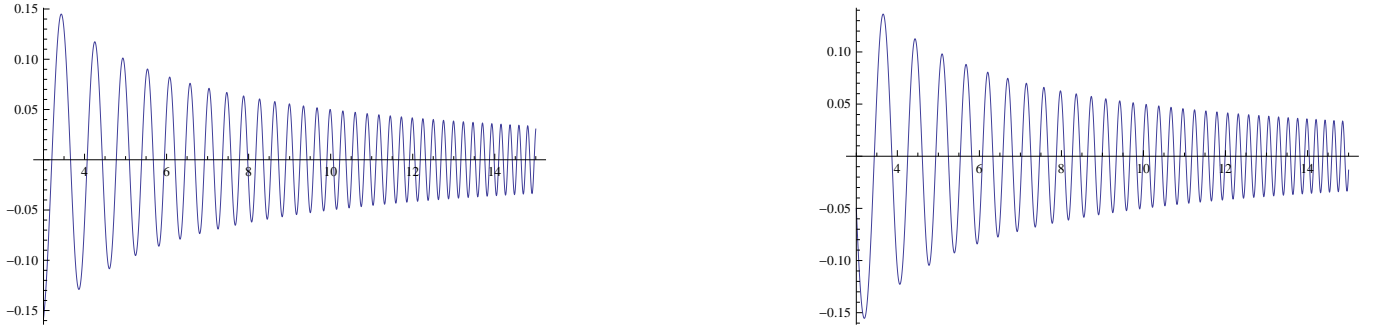


Figure S5: The same as in Fig.S4 but for $\theta = \pi/4$. Both $\text{Re}J_c$ and $\text{Im}J_c$ rapidly oscillate with R . We verified that oscillations persist for all $\theta < \pi/2$. The value of R at which oscillations begin gets progressively larger as θ increases and diverges at $\theta \rightarrow \pi/2$

The issue then is to calculate J_c . It is a complex function $J_c = \text{Re}J_c + i \text{Im}J_c$, whose real and imaginary parts are given by

$$\begin{aligned} \text{Re}J_c &= -2R \int_0^{\delta/2} e^{-(R^2 \cos 2\theta)/(2u_m)} \sin(\theta - R^2 \sin 2\theta) d\theta \\ \text{Im}J_c &= 2R \int_0^{\delta/2} e^{-(R^2 \cos 2\theta)/(2u_m)} \cos(\theta - R^2 \sin 2\theta) d\theta \end{aligned} \quad (\text{S45})$$

At δ exactly equal to π , both terms can be readily calculated numerically. We show the results in Fig.S4. While the real part $\text{Re}J_c$ rapidly approaches $-\sqrt{2\pi u_m}$, the imaginary part $\text{Im}J_c$ rapidly approaches $(2u_m/R)e^{R^2/(2u_m)}$. As a result, $\Lambda_\pi \approx (2u_m/R)e^{R^2/(2u_m)}$, which is nothing but $2 \int_0^R dy e^{y^2/(2u_m)}$. Obviously, Λ_π diverges when $R \rightarrow \infty$.

We found that the behavior of $\text{Re}J_c$ and $\text{Im}J_c$ changes qualitatively at large R once δ becomes different than π (see Fig. S5). In particular, starting from some critical R_0 , both $\text{Re}J_c$ and $\text{Im}J_c$ become oscillating functions of R . As a result, there is an infinite set of R_i at which $\text{Re}J_c = 0$ and an infinite set of R_j at which $\text{Im}J_c = 0$. We show this behavior in Fig. S5 for $\delta = \pi/2$. The value R_0 at which oscillations begin is infinite at $\delta = \pi$, but is finite at any $\delta < \pi$ and its value decreases as $\pi - \delta$ increases.

Because both $\text{Re}J_c$ and $\text{Im}J_c$ oscillate, the limit of each of these functions at $R \rightarrow \infty$ depends on how one approaches $R \rightarrow \infty$. In particular, one can use the fact that there is an infinite set of R 's for which $\text{Re}J_c = 0$, $\{R_i\}$, and another

one for which $\text{Im}J_c = 0$, $\{R_j\}$. By approaching the limit $R \rightarrow \infty$ via the sets $\{R_i\}$ and $\{R_j\}$, we obtain $\lim_{R \rightarrow \infty} J_c = 0$. We emphasize that this is only possible for $\delta < \pi$, when both $\text{Re}J_c$ and $\text{Im}J_c$ oscillate with R . Substituting $J_c = 0$ into (S44) we find

$$\Lambda_\delta = e^{-i\delta/2} \sqrt{2\pi u_m} \quad (\text{S46})$$

Hence, $\Lambda_\pi = \lim_{\delta \rightarrow \pi} \Lambda_\delta = -i\sqrt{2\pi u_m}$, i.e. it is finite. Note that Eq. (S46) gives the same result for Λ_δ which we would obtain by formally substituting $u_m \rightarrow u_m e^{-i\delta}$ into Eq. (S35). For other ways to regularize such an integral see Refs. [6, 7].

The same computational scheme can be applied to the evaluation of the action near the extremum of $S_{\text{eff}}[\psi, \varphi]$. Taken as a function of ψ , the extremum is a maximum rather than a minimum. Expanding the action near the maximum at $\psi = \psi_0$, we get $S_{\text{eff}}[\psi, \varphi] = S_{\text{eff}}[\psi_0, \varphi] - A(\psi - \psi_0)^2$ with $A > 0$. For the partition function, we then obtain

$$Z = Z_0 \int d\psi e^{A(\psi - \psi_0)^2} \quad (\text{S47})$$

Formally, the integral diverges and makes the expansion near ψ_0 problematic. However, once we define the integral over ψ in the same way as above, the integral becomes finite and one can apply a conventional reasoning (e.g., large N expansion [5]) to justify the approximation in which $S_{\text{eff}}[\psi, \varphi]$, viewed as a function of ψ , is taken at the maximum.

-
- [1] S. Maiti and A. V. Chubukov, Phys. Rev. B **82**, 214515 (2010).
 - [2] R. M. Fernandes, A. V. Chubukov, J. Knolle, I. Eremin, J. Schmalian, Phys. Rev. B **85**, 024534 (2012).
 - [3] S. Maiti and A.V. Chubukov, Phys. Rev. B **83**, 220508 (2011).
 - [4] A. B. Vorontsov, M. G. Vavilov, and A. V. Chubukov, Phys. Rev. B **81**, 174538 (2010).
 - [5] S. Sachdev, *Quantum phase transitions*, Cambridge University Press, 2011.
 - [6] J. S. Langer, Ann. of Phys. **41**, 108 (1967).
 - [7] Hagen Kleinert, *Path Integrals in Quantum Mechanics, Statistics, Polymer Physics, and Financial Markets*, World Scientific Publishing Company, 2006.
-